ELSEVIER

Deep-Sea Research II 51 (2004) 2003–2022

DEEP-SEA RESEARCH
PART II

www.elsevier.com/locate/dsr2

A model study of circulation and cross-shelf exchange on the west Antarctic Peninsula continental shelf

Michael S. Dinniman*, John M. Klinck

Center for Coastal Physical Oceanography, Old Dominion University, Norfolk, VA 23529, USA

Accepted 10 July 2004

Abstract

Exchange of warm, nutrient-rich Circumpolar Deep Water (CDW) onto Antarctic continental shelves and coastal seas has important effects on physical and biological processes in these regions. The present study investigates the locations of this exchange and their dynamics in the west Antarctic Peninsula with a high-resolution three-dimensional numerical model. The model circulation is forced by daily wind stress along with heat and salt fluxes calculated by bulk formulae. All surface fluxes are modified by an imposed climatological ice cover.

The model circulation compares favorably to general schematics of the flow based on dynamic topography, water properties from recent hydrography, and ADCP measurements. The sea-surface temperature is similar to satellite estimates except that the model temperatures are slightly higher than observations in the summer and lower in the winter. The seasonal variation of the depth and temperature of the model mixed layer matches observations reasonably well. Sub-pycnocline temperature shows evidence of persistent intrusion of warm CDW onto the shelf, for example, at the shelf break offshore of Adelaide Island. There is a significant correlation between the curvature of the shelf break and the volume transport across the shelf break, indicating that circulation crosses the shelf break in places where the tendency of the flow to maintain a given direction would have it cross a strongly curved bathymetric contour. A momentum term balance shows that momentum advection helps to force flow across the shelf break in specific locations due to the curvature of the bathymetry. For the model to create a strong intrusion of CDW onto the shelf, it appears two mechanisms are necessary. First, CDW is driven onto the shelf at least partially due to momentum advection and the curvature of the shelf break. Then, the general shelf circulation pulls the CDW into the interior.

1. Introduction

The Southern Ocean is a heterogeneous system composed of a variety of sub-regimes, each with its own characteristic physical, biological and chemical features (Tréguer and Jacques, 1992). For

*Corresponding author. Tel.: +1 757 683 5559; fax: +1 757 683 5550.
E-mail address: msd@ccpo.odu.edu (M.S. Dinniman).

0967-0645/$ - see front matter © 2004 Elsevier Ltd. All rights reserved.
doi:10.1016/j.dsr2.2004.07.030

example, the West Antarctic Peninsula (WAP) region is thought to have little or no bottom water formation, large populations of Antarctic krill (*Euphausia superba*) and an active circulation including interactions with the southern boundary of the Antarctic Circumpolar Current (ACC) (Marr, 1962; Hofmann et al., 1996; Hofmann and Klinck, 1998a). In contrast, the Ross Sea produces bottom water (although the amount is uncertain), is the most biologically productive region of the Antarctic, and has generally sluggish sub-tidal circulation (Arrigo et al., 1998; Jacobs and Giulivi, 1998). In order to address fundamental questions on the controls of phytoplankton productivity and growth in these two systems, a suite of physical and biological models is being developed and used in both locations (Dinniman et al., 2003; Smith et al., 2003). Physical forcing, which includes advective circulation, vertical mixing, vertical stratification, and irradiance availability, may be the primary factor producing the observed vertical and horizontal variability in phytoplankton distribution and primary production in the WAP region. Oceanic Circumpolar Deep Water (CDW), a relatively warm, salty and nutrient-rich water mass that is part of the ACC, flows along the shelf break in the WAP region. This water occasionally intrudes onto the continental shelf (Hofmann and Klinck, 1998a) where it moderates the ice cover through heat flux, provides a relatively warm subsurface environment for some animals, and provides nutrients to stimulate primary production (e.g., Prézelin et al., 2000). CDW exchange is known to be episodic, but persistent, and is thought to occur at specific locations due to bottom topography. This study analyzes the exchange of CDW.

The WAP region has been studied intermittently for many years with an accumulated understanding of the physics, chemistry and biology in the area (cf. Ross et al., 1996; Hofmann et al., 2004). The area contains a relatively deep continental shelf (200–500 m) about 200 km wide with rugged bottom topography. The major circulation features in the WAP shelf area are the northeasterly flowing ACC close to the shelf break and a southward flowing coastal current (Hofmann et al., 1996; Klinck et al., 2004). The coastal current is thought to turn into and flow cyclonically around Marguerite Bay. ADCP measurements (S.L. Howard, personal communication) as well as satellite-tracked drifters (Beardsley et al., 2004) also show a current turning into Marguerite Bay just south of Adelaide Island and flowing clockwise around the Bay. Dynamic topography for the WAP shelf suggests that the circulation is largely cyclonic with perhaps one or more subgyres on the shelf (Stein, 1992; Smith et al., 1999; Klinck et al., 2004). The ADCP and drifter measurements also indicate locations where the flow is directed more across the shelf than along it, suggesting gyral circulation on the shelf.

Tidal flow on this shelf is rather weak (a few $cm\,s^{-1}$) based on limited observations and a local tidal model (Padman et al., 2002). Internal tides are thought to be important for straining sea ice (Howard et al., 2004). The continental shelf in this area is mostly ice free in summer and ice covered in winter, with the sea ice developing rapidly from May to July, reaching a peak in August, and declining slowly from September through January (Stammerjohn and Smith, 1996).

The water mass structure on the west Antarctic Peninsula shelf is described in detail in Smith et al. (1999). As a reminder, water structure from top to bottom is composed of Antarctic Surface Water (-1.8 to $1.0\,^{\circ}C$, 33.0–33.7 psu), Winter Water ($-1.5\,^{\circ}C$, 33.8–34.0 psu), and CDW, which has several sub-types. There is no cold, salty, dense water on this shelf of the kind observed in the Weddell and Ross Seas.

Off of the shelf, CDW has two types associated with either a temperature maximum (Upper CDW) with relatively high temperatures (1.6–2.0 °C) or a salinity maximum (Lower CDW) of 34.73. UCDW occupies a depth range of 300–600 m and is relatively easily transported across the shelf break. LCDW occurs between 700 and 1000 m and is less frequently seen on the shelf. A modified (cooled) form of UCDW is seen on the west Peninsula shelf, with temperatures between 1.2 and 1.5 °C and only slightly reduced salinity.

For the purposes of this paper, the temperature of the water below the permanent pycnocline (below 200 m) is a good indicator of recent exchange of CDW across the shelf break. Water

above 1.5 °C is considered to be oceanic water that recently intruded onto the shelf. The rate of cooling of UCDW on the WAP shelf is not known, but measurements from successive cruises (Klinck, 1998) indicate that 2–3 months is enough to convert UCDW into modified CDW.

The goal of this study is to examine the exchange between the shelf and the open ocean as part of a larger effort to determine the effect of circulation and nutrient dynamics on phytoplankton growth on Antarctic continental shelves. A finite difference primitive equation model is used to simulate the circulation in the WAP region in order to analyze the cross-shelf-break exchange of CDW. Several results from the model are compared to different observations to show the validity of the model for examining the cross-shelf-break physics. These results lead to a discussion of the cross-shelf-break heat, salt and volume transport.

2. Model configuration

The Rutgers/UCLA Regional Ocean Model System (ROMS) was used for this study. The model domain (Fig. 1) is located along the west side of the Antarctic Peninsula from about 70°S to just past the northern tip, covers the entire continental shelf and extends ≈ 500 km seaward of the shelf break. The eastern boundary of the model is a closed solid wall (no direct connection to the Weddell Sea) with a free-slip condition. All the other three boundaries are partially or completely open, depending on the coastline (Fig. 1). The horizontal grid spacing (5 km) was chosen to allow as much topographic detail as possible. A dynamic vertical mode calculation based on horizontally averaged density from measurements on this shelf results in a first internal radius of deformation of 4.7 (winter) to 5.3 km (fall). The model marginally resolves baroclinic eddies for this region. There are 24 vertical levels that are concentrated towards the top and bottom of the model domain. The gridded bathymetry used is derived from the Smith and Sandwell (1997) ETOPO2 global 2 min resolution bathymetry with modifications made around Marguerite Bay based on chart data (R.C. Beardsley, personal communication). The bathymetry is artificially "straightened" for the last few grid-points (isobaths set normal to the boundary) at every open-boundary to improve performance of open-boundary conditions. The bathymetry was somewhat smoothed with a modified Shapiro filter which has been designed to selectively smooth areas where the changes in bathymetry are large with respect to the total depth (Wilkin and Hedström, 1998). Therefore, much of the smoothing was on the shelf and there was less smoothing over the shelf break. The model setup is similar to that for the circulation model of the Ross Sea described in Dinniman et al. (2003) and several other details are described there.

Open boundaries use a two-dimensional radiation scheme combined with adaptive nudging (Marchesiello et al., 2001), except for the temperature and salinity. Several radiation schemes were tried for the tracers on the open boundaries, and all of them had problems where the shelf-break intersected the northern boundary. Instead, the temperature and salinity were relaxed to values from the World Ocean Atlas 98 (WOA98) climatology over the 10 grid points closest to the open boundary using the flow relaxation scheme of Martinsen and Engedahl (1987). The model setup at the boundaries for the velocities differed from that in Marchesiello et al. (2001) for their US West Coast experiment only in that no nudging is used for the baroclinic velocities and the component of the barotropic velocity parallel to the boundary, τ_{out} (the time scale for nudging for outgoing waves) is 4 years and τ_{in} (the time scale for nudging for incoming waves) is 4 years/30 ($= 48.7$ days). The barotropic velocities were relaxed to monthly values of depth-averaged circulation from the Parallel Ocean Circulation Model (POCM) global 0.25° resolution model (Semtner and Chervin, 1992).

The model is initialized with horizontally uniform temperature and salinity and a vertical structure obtained from the average of the WOA98 values in the model domain. In order to lessen the shock from the initial geostrophic adjustment, the horizontal variation is ramped in by running the model for five days with the

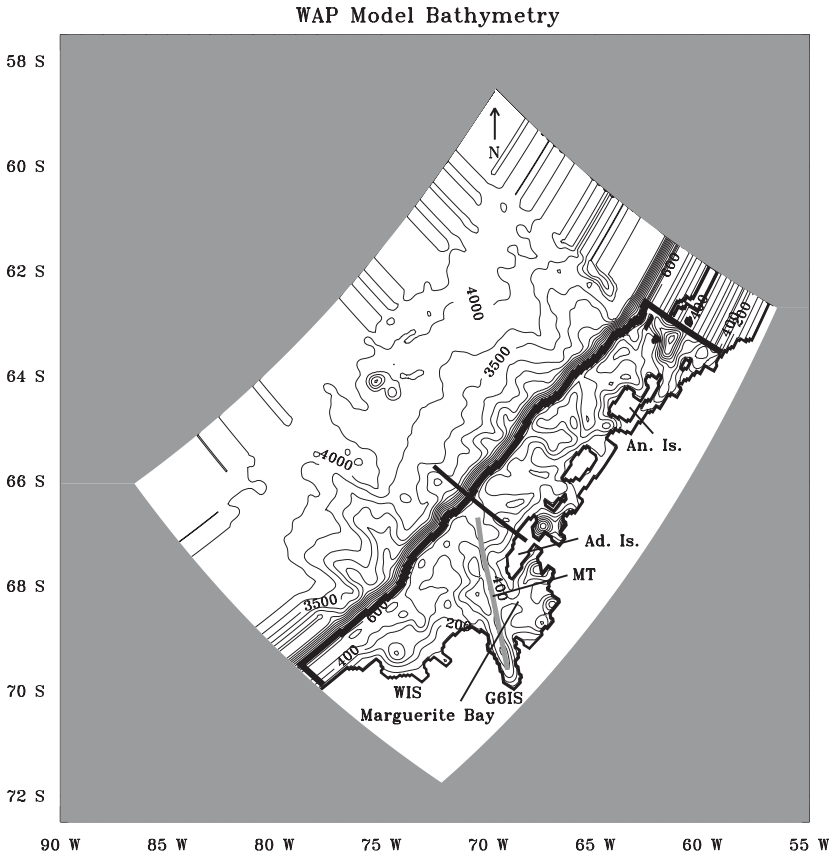

Fig. 1. Model domain and bathymetry. The contour interval for the bathymetry is 50 m up to 1000 m depth and 250 m below 1000 m. 'Ad. Is.' is Adelaide Island and 'An. Is.' is Anvers Island. The solid line from Adelaide Island across the shelf break represents the section covered in Fig. 9. The thick line around the shelf represents the enclosed shelf region discussed in Section 4.1. The line in Marguerite Bay labeled 'MT' shows the location of the Marguerite Trough. 'G6IS' shows the location of the George VI Ice Shelf and 'WIS' represents the Wilkins Ice Shelf.

stratification strongly relaxed to the gridded temperature and salinity climatology. The nonlinear equation of state is used. Silicate, nitrate and chlorophyll are also simulated in the model as passive tracers but will not be discussed here.

Daily values of wind stress and wind speed were obtained from a blend of NSCAT and ERS-2 scatterometer data and NCEP analyses to give a repeatable annual cycle from August 1996 through July 1997 (Milliff et al., 1999). The wind stress is applied as a body force over the top three layers of the model. Instead of using a fully dynamic sea-ice model, ice concentrations from a climatology derived from the special sensor microwave imager (SSM/I) are imposed. The model surface heat flux is then calculated as a linear combination of heat flux due to ice cover and the open-water heat flux with the ratio determined by the ice concentration in that grid cell (Markus, 1999). The open-water heat flux was calculated with the COARE bulk flux algorithm (Fairall et al., 1996), with most of the necessary atmospheric data coming from monthly climatologies from either the NCEP reanalysis (air pressure, humidity and air temperature) or the ISCCP cloud climatology. Daily winds were used for the open-water heat flux calculation. The model surface freshwater flux (imposed as a salt flux) is also calculated as a linear combination of open-water evaporation minus precipitation and that due to ice melting or freezing (Markus,

1999). Precipitation was taken from the Xie and Arkin (1997) climatology. There is no relaxation term for the surface temperature or salinity except at the open boundaries. None of the cavities under ice shelves in the region (primarily the George VI and Wilkins Ice Shelves) are included.

ROMS has a terrain following vertical coordinate system, and these types of models have a well-known problem with their discrete approximation of horizontal pressure-gradient force (Haney, 1991; Mellor et al., 1994, 1998; Song, 1998; Shchepetkin and McWilliams, 2003). A large error was not expected here due to the relatively weak stratification in much of the model domain, and a simple experiment verified this. A simulation was run with the model initialized with a representative vertical temperature and salinity profile with no horizontal variability and all the surface fluxes and boundary relaxation terms set to zero. The resulting flow should be zero, so that any circulation is due, at least initially, to errors due to the vertical discretization (pressure gradient, non-uniform vertical mixing, etc.). As expected, the error flow is very small. After 5 days, the rms velocity for the entire model domain is $0.18\,cm\,s^{-1}$ (maximum: $2.5\,cm\,s^{-1}$) compared with $6.57\,cm\,s^{-1}$ (maximum: $66.9\,cm\,s^{-1}$) for the forced flow.

After the 5-day spin-up of the stratification, the model is initialized to start in late austral winter (September 15). Model simulations have been run successfully for slightly longer than two years and all results presented here will be from the second year unless explicitly stated otherwise.

3. Results

3.1. Circulation

The model circulation along the outer shelf must be representative of the observations if this model is to be used to study the interaction of the shelf and the open ocean. The circulation on the shelf in the west Antarctic Peninsula region is usually described in terms of the northeasterly flowing ACC along the shelf break and a southward flowing coastal current with perhaps some gyral circulation between the two. However, it has also been suggested that the shelf circulation is not coherent over large distances (Hofmann and Klinck, 1998a), but instead is composed of localized gyres with length scales that appear to be determined by the rugged bottom topography. In order to estimate the circulation below the surface, a map of ADCP measurements (see Howard et al., 2004, for details on the ADCP data) at 200 m was made (Fig. 2). The ADCP data come from seven cruises during austral fall and winter of 2001 and 2002 as part of the Southern Ocean Global Ecosystem Dynamics (SOGLOBEC) program (Table 1). All the available 1-h measurements at the appropriate depth bin from all seven cruises were simply averaged in 0.50° longitude by 0.20° latitude boxes (approximately 22 km on a side). This is obviously not a synoptic picture, but it can give an idea of the sub-surface circulation in this area. The flow along the shelf break is primarily, although not exclusively, to the northeast with large velocities that may indicate the ACC against the shelf break. There is a weak indication of a coastal current to the south along Adelaide Island, although it is much more visible at 50 m (not shown) implying that the coastal current is a surface feature. Beardsley et al. (2004) also suggest that the coastal current is at least "surface-intensified". There is a noticeable circulation turning into the north side of Marguerite Bay along the north side of Marguerite Trough (MT), flowing cyclonically around the depression in the mouth of the bay and back out on the south side of the Trough. There are also several other small-scale circulation features on the shelf. For example, note the cyclonic circulation around trenches that open up into the shelf break at 66.5° and 65.1°S with flow onto the shelf on the north side and off the shelf on the south.

A temporal average of the model circulation over mid-March–mid-September of year 2 (model days: 550–730, Fig. 3) shows the flow over the shelf to be similar to the estimated circulation. Much of the model flow is constrained to follow bottom topography. Point comparisons of flow vectors are problematic because the small scale and strongly topographically forced nature of the flow means than small errors in the modeled topography can lead to large differences in flow velocity at a

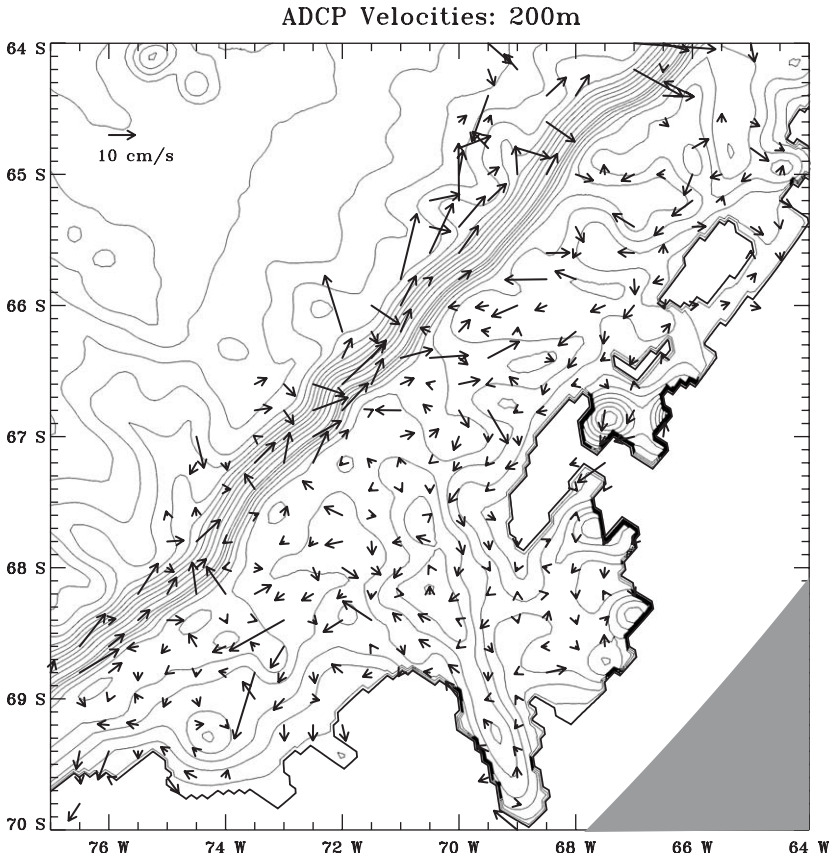

Fig. 2. ADCP measurements of velocity at 200 m along the WAP shelf from seven cruises during austral fall and winter (see text). The bathymetry is that used in the model and the contour interval is the same as for Fig. 1.

Table 1
S.O. GLOBEC cruises that produced ADCP data used here

Cruise	Date
NBP0103	Apr 23–June 6 2001
NBP0104	July 21–Sept 6 2001
LMG0103	Mar 18–Apr 13 2001
LMG0104	Apr 23–June 6 2001
LMG0106	July 21–Sept 6 2001
NBP0202	Apr 9–May 21 2002
NBP0204	July 31–Sept 18 2002

LMG—R/V Laurence M. Gould. NBP—R/V Nathaniel B. Palmer.

specific location. Also, the time scales of the measurements are quite different. With these in mind, the comparison to actual ADCP measurements is quite reasonable. There is a current to the northeast along the shelf break, although the velocities along the break itself are a little weak (compared to the ADCP data) with the model ACC core located off the shelf break. The model does not have an average southward coastal current along Adelaide Island, although (not shown) one does show up from time to time depending on the local winds. A possible reason for this could be that the model does not have accurate fresh water processes at the coastal boundaries, and it is known that this can be very important dynamically at high latitudes (Royer, 1998; Bacon et al., 2002). Large quantities of fresh water enter the system from the melting of glaciers and ice sheets in the area. For example, the net freshwater flux from basal melting of the George VI Ice Shelf into the sound directly beneath it has

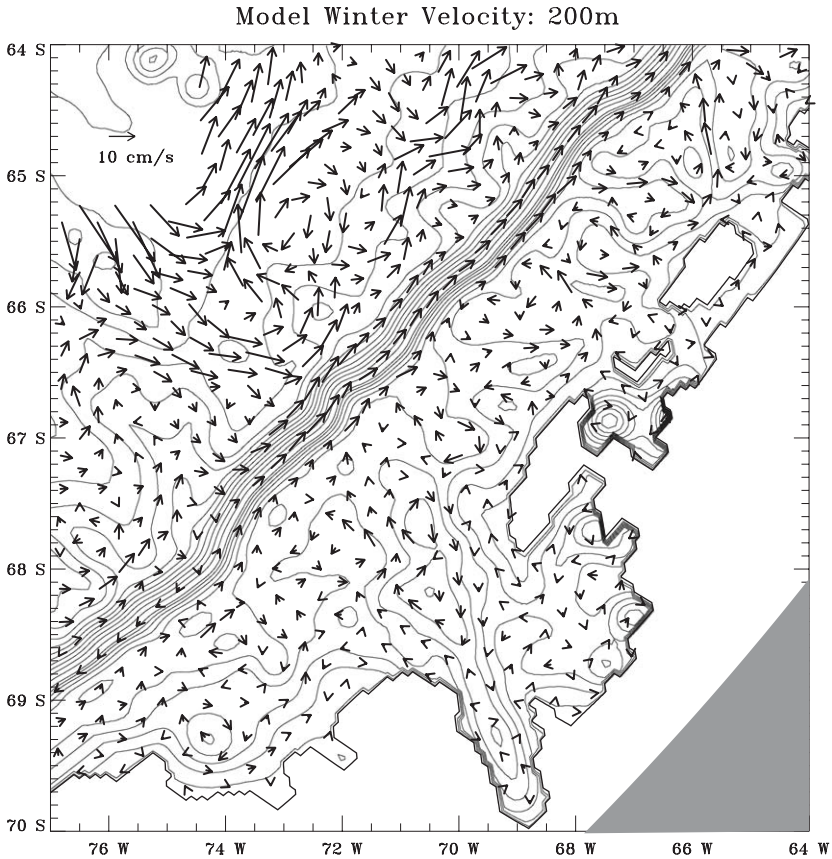

Fig. 3. Total flow at 200 m averaged over model day 550–730 (mid-March–mid-September of year 2). The contour interval for the bathymetry is the same as for Fig. 1. Every fourth model vector is plotted.

been estimated to be 2.1 m year^{-1} (Potter and Paren, 1985). The coastal current in the model should be significantly improved by having more realistic fresh water sources near the coast, especially freshwater melt from ice shelves and we plan to add this in the future.

The model does have a current turning into the north side of Marguerite Bay along the north side of the trench, flowing cyclonically around the depression in the mouth of the bay and back out on the south side of the bay very similar to that in the observations. It appears that in both the model and the observations much of the water flowing into the north side of Marguerite Bay comes from the north side of the MT at 66.5°S. The flow into and around the trenches that cut into the shelf at 66.5° and 65.1°S is also very similar to the ADCP data. It is this cross-shelf circulation near the shelf break that will be important for CDW intrusions.

In order to make a more quantitative comparison between the ADCP observations and the model output, the model velocities were horizontally averaged into the same boxes as the measurements and then compared in any box where there were observations. The comparison was done at 200 m to remain below the layer directly forced by the wind, thus avoiding oscillations in the measured velocity due to wind variability. Although the ADCP measurements were taken over several months, most of the horizontal boxes only have measurements from one or two individual cruises. Therefore, it is more appropriate to use snapshots of the model velocity for the comparison instead of using a temporal

average even though no individual snapshot will be representative of the time period over which the observations were gathered. The mean ADCP velocity at the comparison points at 200 m was 7.3 cm s^{-1}. A comparison was made using snapshots every 10 days over mid-March–mid-September of year 2 (model days: 550–730). The average model velocity magnitude at the same points was a little less than observations (6.4 cm s^{-1}) with an average difference between the two of 0.9 cm s^{-1} and an average rms error of 6.8 cm s^{-1}.

The intrusion of CDW onto the west Antarctic Peninsula continental shelf has been consistently observed to occur at specific locations over the years. For example, the maximum temperature (below the surface layer) observed over the shelf for the period Apr 23–June 6, 2001 (Fig. 4) shows a strong plume of intruding warm CDW along the north side of MT northwest of Adelaide Island. Warmer water also can be seen going into Marguerite Bay. There is a second possible intrusion across the center of the grid, but the signature is weak. Klinck et al. (2004) estimate that 4–6 intrusions of CDW occur per year on this part of the WAP continental shelf, with the water moving on the shelf at a speed of about 2.5 cm s^{-1}. Episodic intrusions also occur in the model. For example, 3–5 (depending on the level of the temperature anomaly that defines an intrusion) separate intrusions can be found in the same area in the model during model year 2. In late August of model year 2 (Fig. 5) an intrusion of CDW can

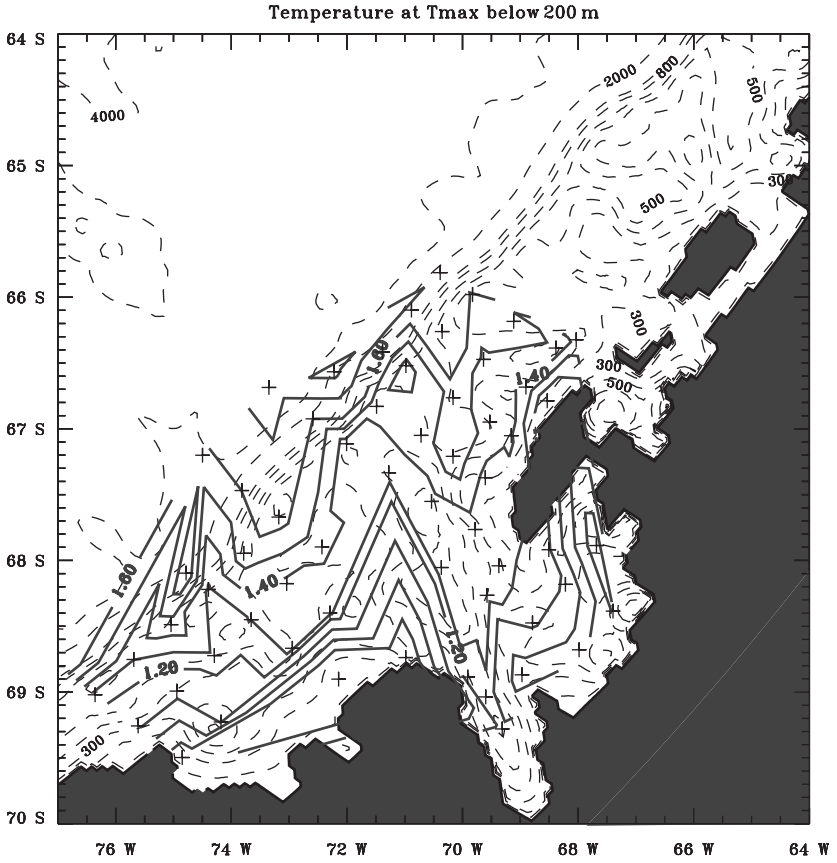

Fig. 4. Distribution of the temperature maximum (°C) below 200 m constructed from CTD temperature observations during May, 2001. The crosses represent station locations. The contour interval is 0.2 °C except between 1.2 and 1.6 °C where it is 0.1. The thin dotted lines in the background are model bottom topography.

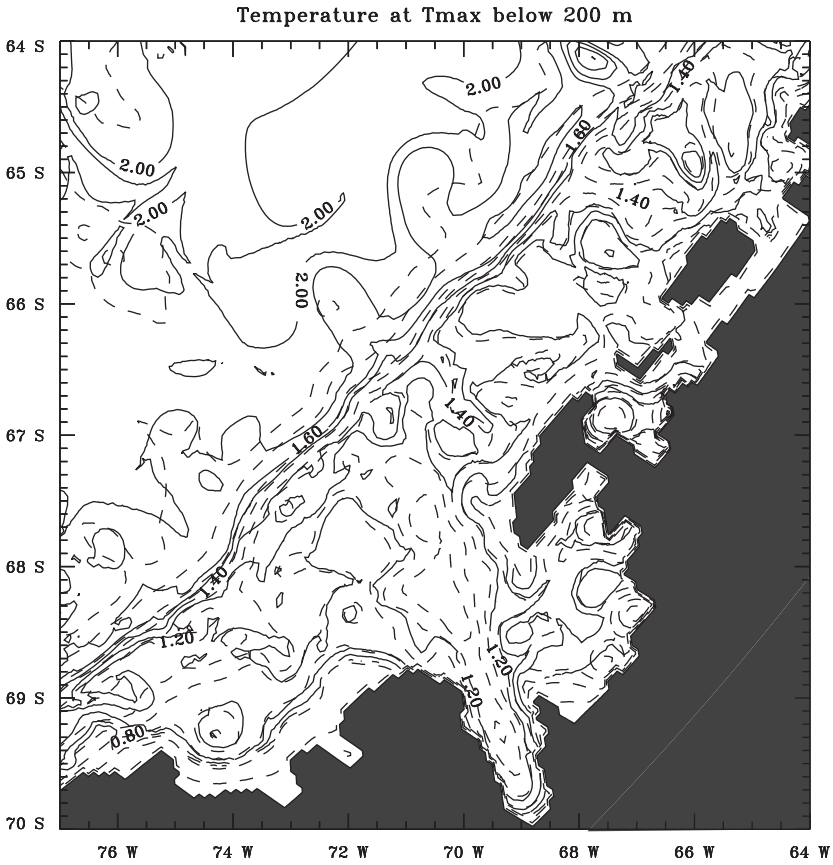

Fig. 5. Model maximum temperature (°C) below 200 m at model day 710 (late August). The contour interval is the same as for Fig. 4.

clearly be seen in the same location (north side of MT) where it occurs in the observations. The influence of the circulation into Marguerite Bay can also be seen in the maximum temperature.

3.2. Temperature

In order to use the model to assess the importance of cross-shelf-break transport on heat budgets on the shelf, it is necessary to examine how well the model is moving heat between the atmosphere, the surface ocean and the interior. One test of the accuracy of the model's surface processes is a comparison of the model sea-surface temperature (SST) to satellite estimates. Since there is no relaxation to a pre-defined temperature, SST accuracy is a check on several processes including the open-water surface heat flux, heat transfer between the ice and the water, penetration of the solar heating below the surface, horizontal advection and vertical mixing.

A climatology of Advanced Very High-Resolution Radiometer (AVHRR) satellite SST covering 1985–2000 with 9 km resolution, averaged over 5-day periods (Casey and Cornillon, 1999) and interpolated onto the model grid, is compared to model SST. Most of the model domain is ice free in austral summer, and much of it has high ice concentrations in winter leading to significant surface temperature changes ($>3.0\,^{\circ}C$ for 85% of the model grid) over the year. The model SST displays mesoscale variability (Fig. 6) that is not apparent in the observed climatology. However, the model SST has a realistic seasonal cycle when compared with the satellite estimates (Figs. 7 and 8). To quantify the SST comparison, the model

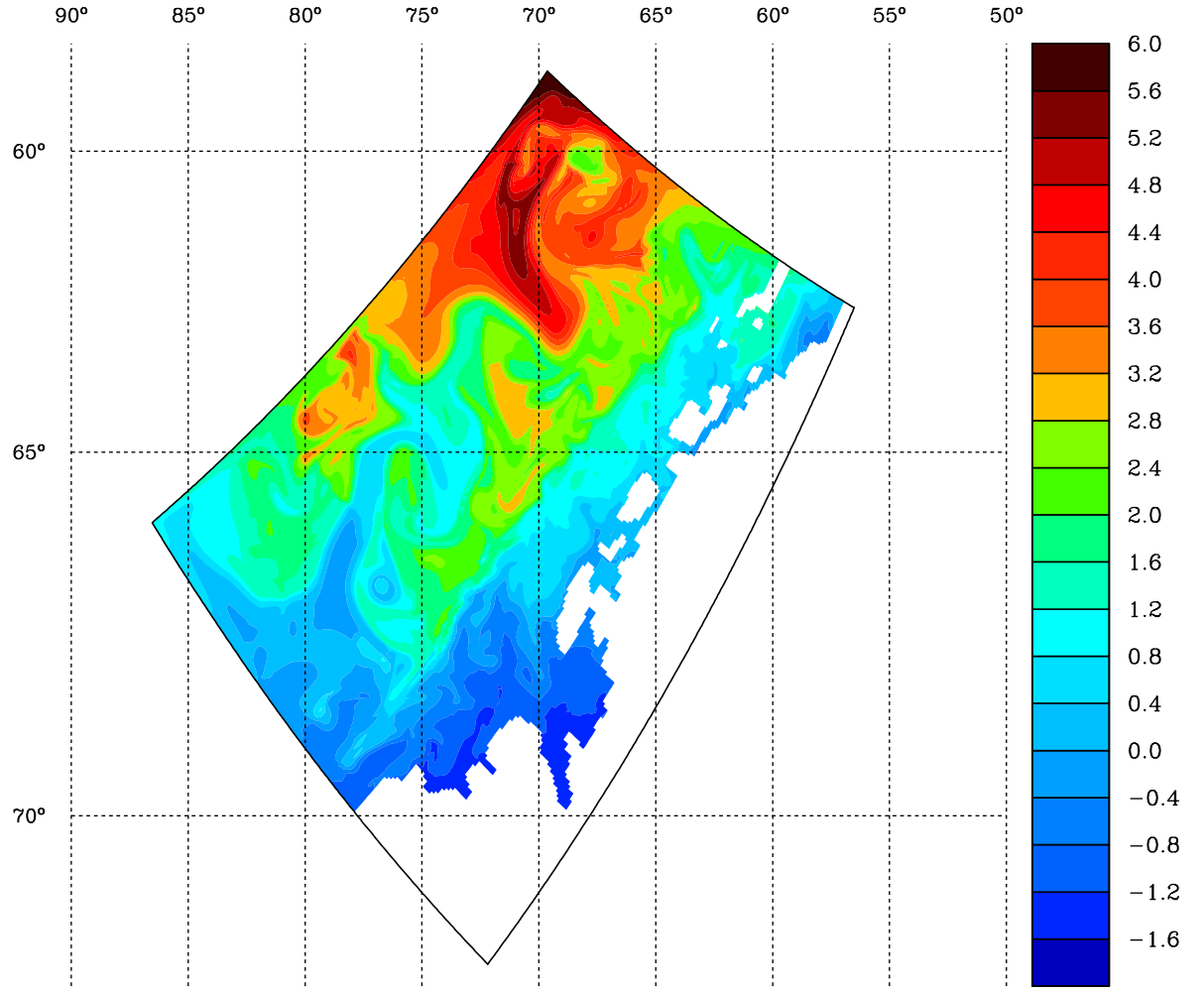

Fig. 6. Model top layer temperature (°C) at model day 510 (February 6).

values for the second year of the simulation are compared to observations at every grid point where AVHRR data were available (low or no sea ice) every 10 days. The average rms error over this period was 0.72 °C with a maximum of 0.97 °C in late March. Some of this error is due to the mesoscale variability in the model that is not in the climatology. The errors are somewhat compensated over the model grid at any given time, with the model SST warm in austral spring and late summer (max error 0.56 °C) and slightly cool in winter (max error −0.24 °C). The annual error over the entire year balances out to be only 0.09 °C. Note that it is also thought the AVHRR Pathfinder SST has a cold bias at high latitudes although the amount is uncertain (K.S. Casey, personal communication). In order to obtain an estimate of the scale of the error due to the mesoscale variability, a climatology of the model SST was created over the entire model run (except the first 90 days). Even though the climatology only extends over 2 years, the average rms error was reduced to 0.60 °C, with a maximum of 0.83 °C in mid-April and an annual error over the entire year of only 0.07 °C. The reduction in rms error due to time averaging of the model SST

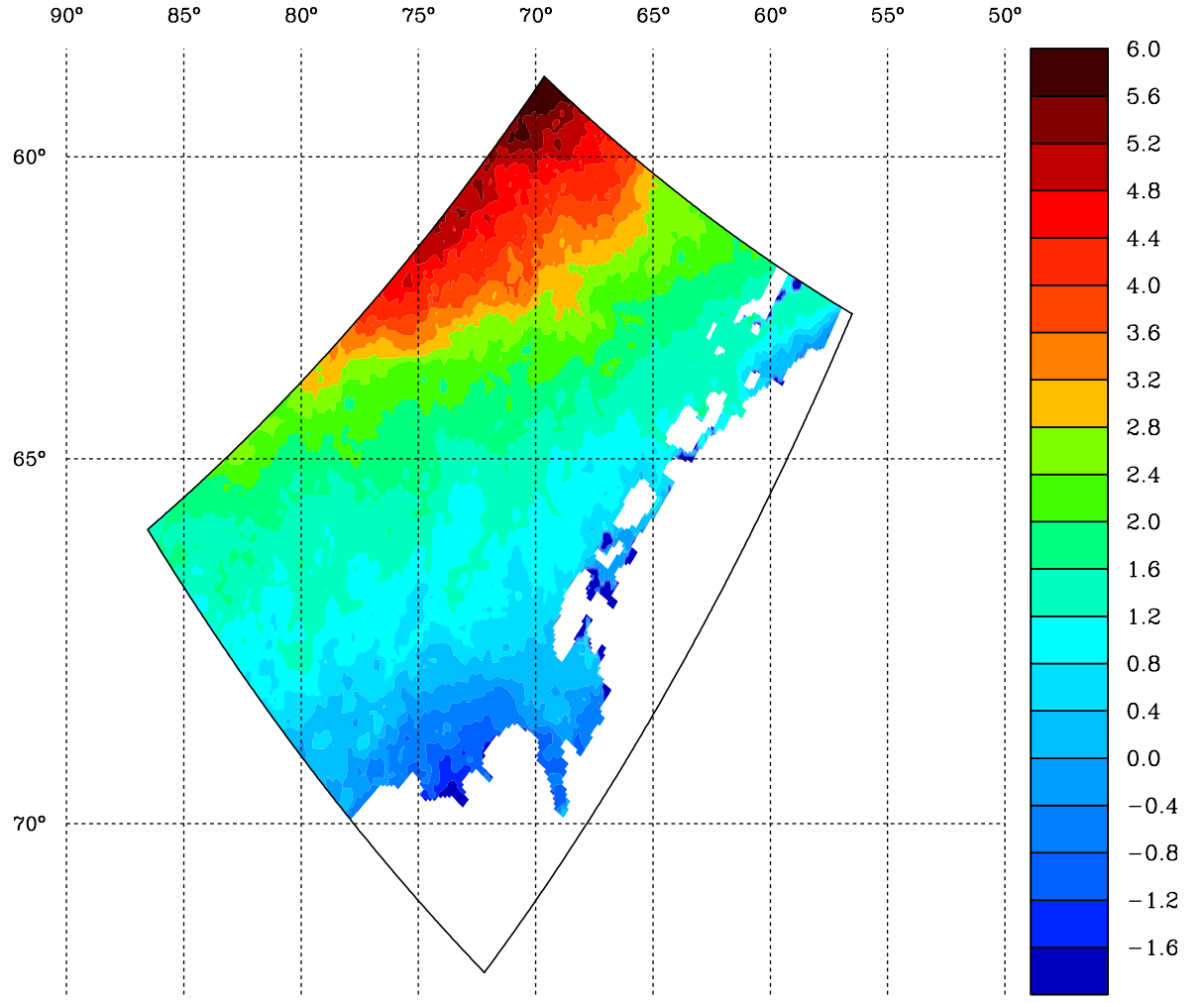

Fig. 7. Satellite (AVHRR) SST (°C) climatology (1985–2000) for the period February 5–9.

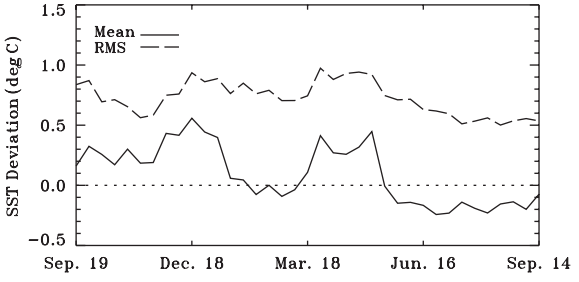

Fig. 8. Comparison between model and AVHRR SST over model year 2. The annual average deviation is 0.09 °C and annual average RMS error is 0.72 °C.

with little change in the mean error indicates that small-scale (mesoscale) variability of the model is the source of much of the rms error.

The model does a reasonable job of estimating the SST. However, two general problems could produce the excess heating in the summer and cooling in the winter. The open-water heat flux formulas were derived for tropical regions and may not be appropriate in high latitudes. Note that different bulk algorithms vary significantly in their calculation of heat flux (Zeng et al., 1998). A related problem could be the cloud-correction algorithm; different cloud-cover algorithms have

a wide variety of effects in the Antarctic (Kim and Hofmann, manuscript in preparation).

The second problem is the magnitude of vertical mixing, which is estimated from a turbulence parameterization (Large et al., 1994). The coefficients in the turbulence model may need to be adjusted for high latitudes and are a current topic of study. Double diffusive mixing, which may (Smith and Klinck, 2002) or may not (Howard et al., 2004) be important, was not used. Tidal mixing, which was not included in the model, can be important in the Antarctic (Levine et al., 1997, Muench et al., 2002) although it is uncertain whether it is significant in the WAP region (Padman et al., 2002; Howard et al., 2004). There also may be problems with the vertical mixing on the inner shelf due to inaccurate surface forcing related to the coast (coastal ice melt and winds). Double diffusive mixing and tidal circulation (driven at the open boundaries) will be added to the model in the future.

Cross sections of the model temperature just north of Marguerite Bay in late January and late July (Fig. 9) show the seasonal cycle of the mixed layer. In late January of model year 2, the temperature matches reasonably well with observations at the same time and location. Water is warmer than 1.25 °C at depth, although the core of the ACC does seem to be farther offshore in the model than in the observations. Cool winter water is centered near 100 m. There is also a shallow layer of warm water at the surface, although the off-shelf surface temperature is too warm (as much as 1 °C) in the model compared to observations. The same section in late July has a 75 m thick very cold mixed layer, with the temperature increasing monotonically with depth below the mixed layer over most of the shelf in both the model and observations. The −1.5 °C contour is at about 80–100 m in both the model and observations while the 0 °C is at 150 m in both. The model does not have the very warm water (>1.75 °C) up against the coast at 200–350 m that appears in the observations. However, the warm water in this location was probably the result of an intrusion of CDW passing by this station. Observations along the same line a couple of months earlier (May 3–4, 2001, not shown) have a maximum temperature of 1.4 °C in the location of the maximum on July 31. The model does show evidence of a intrusion of warm CDW near 350 m.

Note that the temperature of the very cold mixed layer in late July in the model is a couple of deci-degree below freezing. This happens because of the imposed ice cover. The model surface heat flux is calculated as a linear combination of heat flux due to ice cover and the open-water heat flux. The heat flux due to the ice cover is a function of the difference between the mixed layer temperature and the freezing point of sea water (Markus, 1999), which means that this heat flux term will not force the temperature below freezing. However, the open-water heat flux can be strongly negative (heat leaving the water) even with the water at the freezing point. At this location in late July, the imposed sea-ice is not 100%, so the heat flux is a combination of the ice cover term and the open-water flux term. The open-water heat flux here is strongly negative leading to strong cooling. Since the rapid cooling cannot directly lead to ice formation (which would reduce the contribution of the open water term) due to the ice cover being imposed, the surface temperature is cooled excessively. This problem will be fixed by adding a dynamic sea-ice model in the future.

4. Discussion

A primary motivation for this model is the study of exchange of water masses across the shelf break and its effect on biological processes. For example, CDW is shown to be important, due to its temperature, to the reproductive cycle of Antarctic krill (Hofmann et al., 1992). The specifics of cross-shelf nutrient transport, as part of CDW intrusions, are important for biological production (Prézelin et al., 2000). Also, the rate and timing of vertical diffusion providing heat and nutrients to the surface layer affect annual cycles of sea ice and summer production.

4.1. Shelf budgets

In order to study exchange across the shelf break, an enclosed "shelf" is defined by the 1000 m

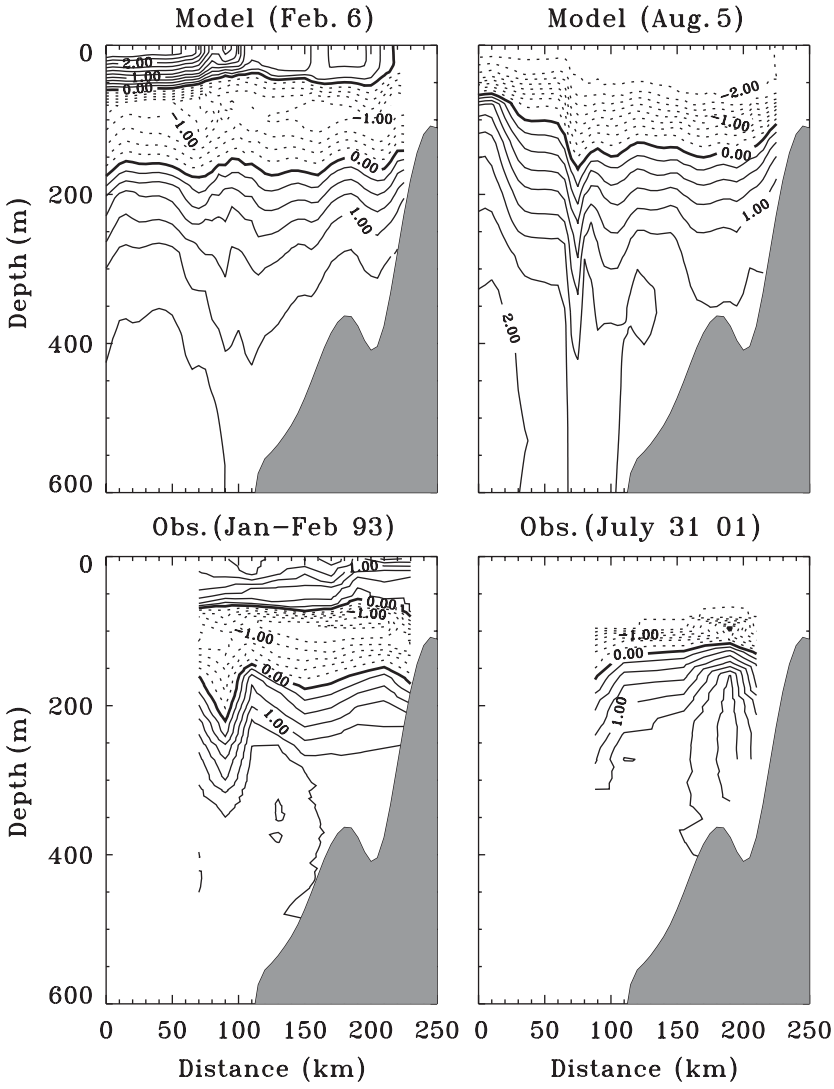

Fig. 9. Modeled and observed temperature cross-sections across the shelf and shelf break across from Adelaide Island (see Fig. 1). The top two figures are from the model at model days 510 (February 6) and 690 (August 5). The bottom two figures are observations from late January to early February 1993 and on July 31, 2001. Temperatures below 0 °C are represented with dashed lines and the contour interval is 0.25 °C.

isobath from near the south end of the model domain to the south end of Bransfield Strait and then to land at each end (Fig. 1). Because of model variability, instantaneous snapshots are not adequate for flux estimates. Instead, accumulated totals of volume and tracer fluxes in each horizontal direction are calculated in the model to increase the accuracy of the computed net flux. A budget of the volume flux onto the shelf computed from 5-day averages over model year 2 shows the mean total transport onto the shelf to be extremely small ($\approx 1400\,m^3\,s^{-1}$ on average). Note that the total horizontal transport onto the shelf does not have to be exactly zero due to the free surface. Although the volume flux is basically zero, there is a small net on-shelf transport of heat

(1.78 TW, heat content here is calculated with respect to the surface freezing point) and salt (0.16 psu-Sv.). If the average temperature (0.7 °C) and salinity (34.5 psu) along the shelf border are used, then the heat flux just due to the mean total transport onto the shelf is 0.014 TW and the salt flux is 0.048 psu-Sv, indicating that the net on-shelf transport of heat and salt is not simply due to the mass imbalance on the enclosed shelf. There is not much of a seasonal signal in the heat flux, instead there are episodic pulses of on and off-shelf heat transport.

The total advective heat flux into the enclosed region normalized by the surface area (1.86×10^{11} m^2) is equivalent to a vertical heat flux of 9.6 W m^{-2}. Using hydrographic observations on and off the shelf from Marguerite Bay north to Anvers Island over 1993 and 1994, Klinck (1998) estimated an annual average equivalent vertical heat flux due to transport of heat across the shelf break in subpycnocline waters to be 4.3 W m^{-2}. The model equivalent salt flux is 0.85 mg salt m^{-2} s^{-1}, while the Klinck estimate is 0.36 mg salt m^{-2} s^{-1}. The model fluxes are within a factor of two of the changes estimated from hydrographic measurements.

The average time rate of change of the heat and salt content on the shelf, normalized by the surface area, can also be computed as an equivalent vertical flux. The change in the heat content in the top 150 m (Fig. 10) shows the expected strong annual cycle with heating in austral spring and early summer and cooling in fall and early winter. However, the annual average change was close to zero (0.3 W m^{-2}). The water below 150 m on the shelf does not have an apparent seasonal cycle and has an annual net loss (2.6 W m^{-2}) of heat, which may be due to winter mixing below 150 m since much of the heat loss occurs in early austral winter. The total change in heat on the shelf is significantly smaller than the advective heat transport onto the shelf.

The change in salt content in the top 150 m on the shelf shows a general trend of freshening in summer and adding salt in fall and winter which is what one would expect from the melting and creation of sea ice. However, there is non-seasonal variability that is due to the precipitation climatology, open-water evaporation, and advection from off the shelf. The annual average increase in the top 150 m is 0.75 mg salt m^{-2} s^{-1}. The change in salt content below the top 150 m is small (annual average 0.07 mg salt m^{-2} s^{-1}), and the annual mean total increase in salt on the shelf (0.82 mg salt m^{-2} s^{-1}) is very close to the total advective transport onto the shelf. For the model, the advective transport is a very important part of the heat and salt budgets on the shelf.

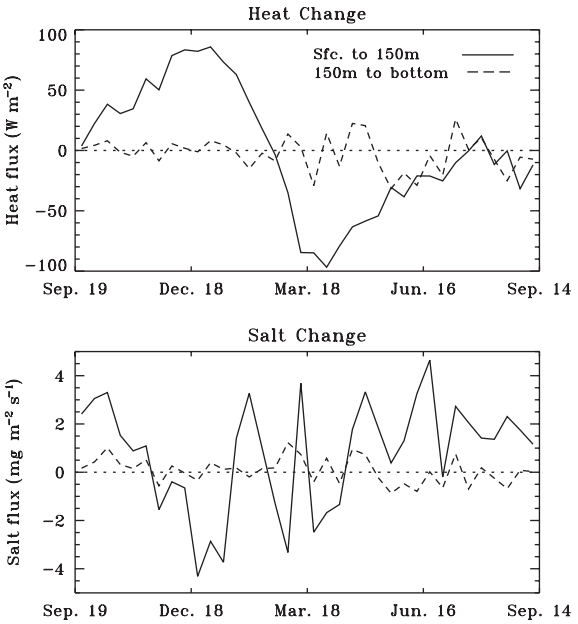

Fig. 10. Time history of change in heat and salt content for the second model year. The two lines in each plot represent the average above and below 150 m for the enclosed area shown in Fig. 1.

There is not much cross-shelf-break transport in either frictional layer represented by the top three model layers (directly forced by the wind stress) or the bottom model layer (over which the bottom friction in the model is directly applied as a body force).

The cross-shelf-break transport of CDW, defined as water below 150 m with a temperature above 1.0 °C, is time variable but averages 0.20 Sv onto the shelf. This water brings in substantial quantities of heat (22 W m^{-2}) and salt (41 mg salt m^{-2} s^{-1}). The equivalent vertical heat and salt fluxes show that advective transport of

CDW is very important to heat and salinity budgets on the WAP shelf. The cross-break transport of CDW accounts for much of the flux below 150 m as the advective heat flux onto the shelf of all waters below 150 m is 25 W m^{-2} and that of salt is 65 mg salt m^{-2} s^{-1}. Much of this on-shelf heat and salt transport is balanced in the model by atmospheric exchange and off-shelf transport of near-surface waters below the top three model layers.

Little Antarctic Bottom Water (AABW) is thought to form in the west Antarctic Peninsula shelf region (Hofmann and Klinck, 1998b; Orsi et al., 1999; Smith et al., 1999). If we define AABW here as water below the permanent pycnocline (150 m) with a temperature below −0.50 °C and a salinity above 34.6 psu, then no Bottom Water is found on or advected onto or off of the shelf.

4.2. Shelf-break exchange processes

Transport of CDW across the shelf break is thought to be tied to certain bathymetric features. For example, a linkage has been proposed between topographically induced upwelling of nutrient-rich CDW (primarily at sites of shallow topography near the shelf break) onto the shelf and the presence of diatom-dominated phytoplankton assemblages on the WAP continental shelf (Prézelin et al., 2000). A cross-section (not shown) of the time-mean cross-slope velocity along a section of the shelf-break across from Marguerite Bay shows the strongest flow generally at the surface, with alternating vertical sections of on and off-shelf transport. The cross-slope velocity at each individual grid point along the shelf break is calculated as

$$U_{\text{cross}} = \vec{U} \cdot \left(\frac{\nabla H}{|\nabla H|} \right),$$

where H is the depth.

Even though the total model cross-shelf volume transport is very close to zero, there are several locations that have relatively large and variable transport consistently on or off the shelf. It appears that many of the locations of cross-shelf transport can be related to the curvature of the shelf break (Fig. 11). This curvature can be numerically computed as the change along the shelf break (where s is the distance along the shelf break) of the unit gradient of the bathymetry:

$$\left| \frac{\mathrm{d}}{\mathrm{d}s} \left(\frac{\nabla H}{|\nabla H|} \right) \right|.$$

The curvature is defined to be positive when, going from southwest to northeast, the shelf-break rotates counter-clockwise. Since the flow along the shelf break is primarily from southwest to northeast, positive curvature rotates the bathymetry so that inertia would tend to drive water onto the shelf. When the annual mean cross-shelf-break volume flux (over model year 2) as a function of position along the shelf break is compared to the curvature (Fig. 12), there is an obvious lagged correlation over much of the shelf break. Note that at the southern end of the shelf break (approximately up to grid index 70), where the volume flux seems to lead instead of lag the curvature, the flow along the shelf break is directed more southwestward (Fig. 3). The correlation is at a maximum at a lag of either 1.5 ($r = 0.481$) or 2.5 ($r = 0.448$) gridpoints, corresponding to 7.5–12.5 km in distance along the shelf break (note that the curvature locations are one-half grid point removed from the cross shelf flow locations). The large-lag standard error (Sciremammano, 1979) is computed to be 0.110, so these correlations are easily statistically significant at the 99% level (2.6σ). Physically, this indicates that circulation crosses the shelf break in places where the tendency of the flow to maintain a given direction would have it cross a bathymetric contour that is rapidly changing direction. The maximum cross-shelf-break flux occurs about 10 km after the maximum change in the shelf-break direction. No significant lagged correlation was found between the cross-shelf-break flux and either the magnitude of the bottom slope or the depth. This indicates that there is no relationship in the model between transport and the depth or sharpness of the shelf break, contradicting earlier suggestions that water moved on the shelf over banks and off the shelf in troughs.

The terms in the momentum acceleration equation were calculated from time-averaged quantities at each level, summed over the entire

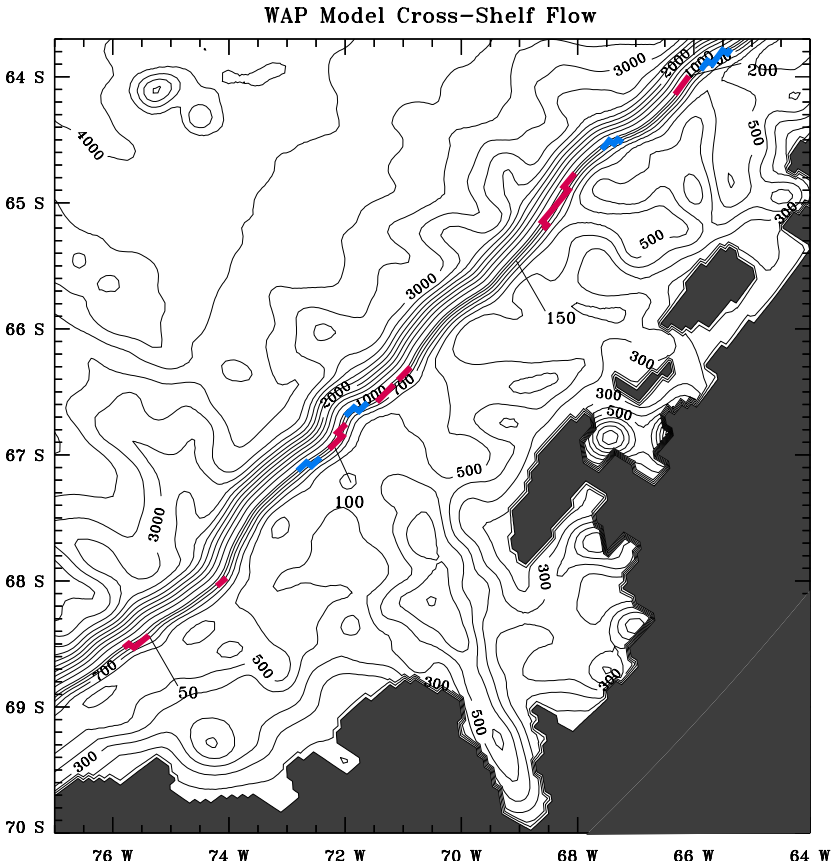

Fig. 11. Magnified view of the model domain and bathymetry around Marguerite Bay. The bathymetry contours are the same as for Fig. 1. Red (blue) lines along the shelf break represent sections where the total cross-shelf-break transport averaged over a year is largely onto (off) the shelf (see Section 4.2). The numbers are indices for a line defined along the shelf break (also see Section 4.2).

water column and then rotated at each grid point into across shelf break and along shelf-break components. Over the shelf break, the dominant terms in the annual average momentum balance in the cross-shelf-break direction are the Coriolis, the pressure gradient force, and the horizontal momentum advection terms, with the surface wind stress contributing but less important. The bottom drag, while important in the bottom boundary layer, does not have a large impact on the vertically integrated cross-shelf acceleration. The momentum advection term is greater than, or at least comparable to, the residual (sum of Coriolis, pressure gradient force, horizontal momentum advection and surface wind stress) over all of the shelf-break edge.

The cross-shelf-break momentum advection term (Fig. 12) is significantly correlated along the shelf break with the cross-shelf-break transport with a lag of either 0 ($r = 0.416$) or 1 ($r = 0.420$) grid points (large-lag standard error 0.124). This implies that on an annual average, some of the forcing of water across the isobaths is due to the non-linear advection of momentum. The momentum advection term is very strongly correlated with the shelf-break curvature ($r = 0.757$), implying that much of the momentum advection in the cross-shelf-break direction is just due to the rotation of the isobaths as one moves along the shelf break. Inertia causes the water to try to travel in a straight line, which will force water onto or off of the shelf when the shelf-break curves. The

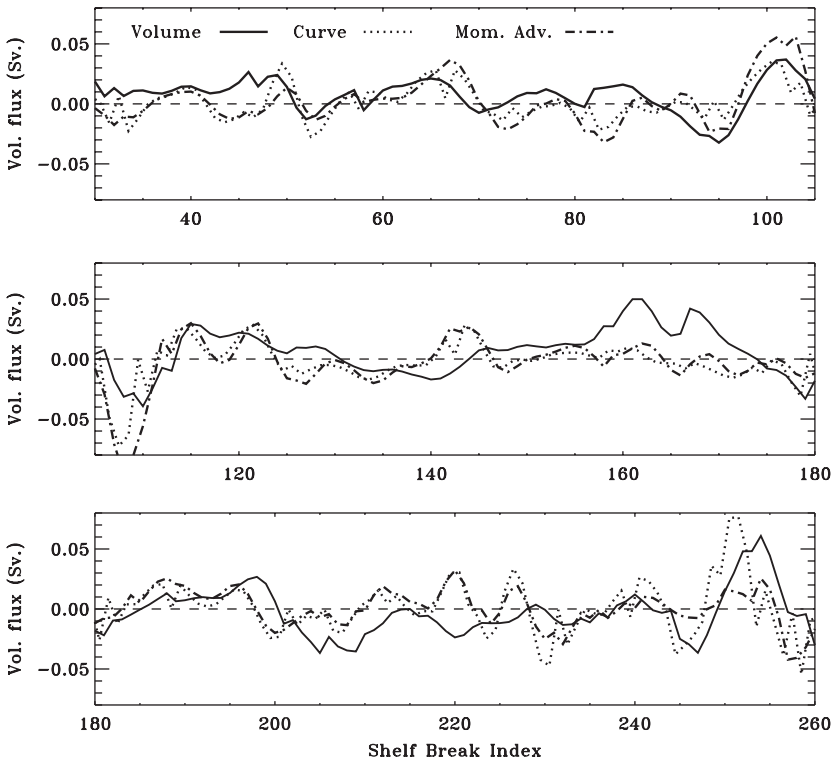

Fig. 12. Cross-shelf-break volume flux (Sv.), shelf-break curvature (normalized units * 0.25) and cross-shelf-break momentum advection term for the entire grid cell volume of water (10^5 m^4 s^{-2}). These are averaged values over model days 365–730. The x-axis is grid number along the defined shelf break.

annual average cross-shelf-break surface Ekman flux (not shown) is primarily on-shore southwest of grid index 180 and offshore to the northeast, and is significantly weaker than the momentum advection term over most of the shelf-break edge. However, there is somewhat of a correlation of surface Ekman flux with the cross-shelf-break transport ($r = 0.375$) along the break that is just barely significant at the 99% level (large-lag standard error 0.131).

Along the shelf break where there is mean on-shelf flow, the deeper CDW driven upward by the shallowing bathymetry raises nutrients that could support a localized increase in biological production. Note that of the four outer shelf-break locations where Prézelin et al. (2000 - Figure 9a) found a diatom-dominated phytoplankton community indicative of nutrient-rich upwelled water, three of them (Prézelin 200, 300 and 600 lines) correspond to locations in this model (shelf edge grid indices 102, 121 and 197) where there is on-shelf flow that is highly correlated to the bathymetric curvature.

However, how many of these locations of strong on-shore flow lead to CDW being transported well onto the shelf? It was noted previously that much of the cross-shelf circulation over the shelf in the model and observations was along bathymetric contours. Warm CDW was shown to intrude onto the shelf in some specific areas (e.g., along the northern side of MT). For example, the on-shelf flux around shelf edge grid indices 115–125 can be carried into the interior of the shelf by the general circulation of the shelf. Note that this is also where the strong intrusion showed up in the observations (Fig. 4). Conversely, the on-shelf flux around indices 85 or 100 does not intrude very far (Fig. 4) because of the mean circulation on the shelf. Also

note that observations show a weak intrusion at this location (index number 85). For the model to create a strong intrusion of CDW onto the shelf, it appears two mechanisms are necessary. Much of the CDW first appears on the shelf due to momentum advection and the curvature of the shelf break. Then, the general circulation on the shelf, which in this case is strongly influenced by bathymetric variations, pulls the CDW into the interior or back off the shelf.

5. Conclusions

A circulation model has been created for the west Antarctic Peninsula region in order to study the exchange of warm nutrient-rich CDW onto the continental shelf in this region. The model circulation is forced by daily wind stress along with heat and salt fluxes calculated by bulk formulae. All surface fluxes are modified by an imposed climatological sea-ice concentration.

The model circulation compares favorably to general schematics of the flow based on dynamic topography, water properties from recent hydrography and ADCP measurements. There are some problems with the circulation in the model near the coast, likely due to incorrect specification of ice-shelf melting. However, the circulation along the shelf break and outer shelf appears to be realistic, which is important for studying the exchange of CDW onto the shelf. The sea-surface temperature is similar to satellite estimates except that the model temperatures are slightly higher than observations in the summer and lower in the winter. Better agreement can be obtained by increasing the mixing across the pycnocline. The seasonal variability of the depth and temperature of the model mixed layer matches observations reasonably well. Sub-pycnocline temperature shows evidence of persistent intrusion of warm CDW onto the shelf, for example, at the shelf-break offshore of Adelaide Island.

Calculations of the advective transport of heat and salt onto the shelf and of the heat and salt budgets on the shelf show that the cross-shelf-break transport of CDW is very important to heat and salinity budgets on the WAP shelf. There is a significant correlation between the curvature of the shelf break and the volume transport across the shelf break, indicating that circulation crosses the shelf break in places where the tendency of the flow to maintain a given direction would have it cross a curving bathymetric contour. A balance of the terms in the momentum equation shows that momentum advection helps to force flow across the shelf break in specific locations due to the curvature of the bathymetry. For the model to create a strong intrusion of CDW onto the shelf, it appears two mechanisms are necessary. First, CDW is driven onto the shelf at least partially due to momentum advection and the curvature of the shelf break. Then, the general circulation on the shelf pulls the CDW into the interior.

Acknowledgements

We thank the Office of Computing and Communications Services at Old Dominion University for the use of the Sun HPC 10000 on which the simulations were run. Comments from Dr. David Musgrave, Dr. Peter Wiebe and an anonymous reviewer were very helpful. Dr. Hernan Arango provided the Beta 1.0 release of ROMS. The AVHRR SST data were provided by Dr. Kenneth Casey. The POCM model output fields were provided by Dr. Ricardo Matano. ADCP data are courtesy of Ms. Susan Howard and Earth and Space Research. Computer facilities and support were provided by the Commonwealth Center for Coastal Physical Oceanography. This work was supported by the US National Science Foundation Grant OCE-99-11731. This is US GLOBEC contribution no. 452.

References

Arrigo, K.R., Weiss, A.M., Smith Jr., W.O., 1998. Physical forcing of phytoplankton dynamics in the western Ross Sea. Journal of Geophysical Research 103, 1007–1022.

Beardsley, R.C., Limeburner, R., Owens, W.B., 2004. Drifter measurements of surface currents near Marguerite Bay on the western Antarctic Peninsula shelf during austral summer and fall, 2001 and 2002. Deep-Sea Research II, this issue [doi:10.1016/j.dsr2.2004.07.031].

Bacon, S., Reverdin, G., Rigor, I.G., Snaith, H.M., 2002. A freshwater jet on the east Greenland shelf. Journal of Geophysical Research 107, 10.1029/2001JC000935.

Casey, K.S., Cornillon, P., 1999. A comparison of satellite and in situ based sea surface temperature climatologies. Journal of Climate 12, 1848–1863.

Dinniman, M.S., Klinck, J.M., Smith Jr., W.O., 2003. Cross shelf exchange in a model of the Ross Sea circulation and biogeochemistry. Deep-Sea Research II 50, 3103–3120.

Fairall, C.W., Bradley, E.F., Rogers, D.P., Edson, J.B., Young, G.S., 1996. Bulk parameterization of air–sea fluxes for Tropical Ocean-Global Atmosphere Coupled-Ocean Atmosphere Response Experiment. Journal of Geophysical Research 101, 3747–3764.

Haney, R.L., 1991. On the pressure gradient force over steep topography in sigma coordinate ocean models. Journal of Physical Oceanography 21, 610–619.

Hofmann, E.E., Klinck, J.M., 1998a. Thermohaline variability of the waters overlying the west Antarctic Peninsula continental shelf. In: Jacobs, S.S., Weiss, R.F. (Eds.), Ocean, Ice and Atmosphere Interactions at the Continental Margin. Antarctic Research Series, vol. 75. American Geophysical Union, Washington, DC, pp. 67–81.

Hofmann, E.E., Klinck, J.M., 1998b. Hydrography and circulation of the Antarctic continental shelf: 150 °E eastward to the Greenwich Meridian. In: Robinson, A.R., Brink, K.H. (Eds.), The Sea, vol. 11. Wiley, New York, pp. 997–1042.

Hofmann, E.E., Capella, J.E., Ross, R.M., Quetin, L.B., 1992. Models of the early life history of *Euphausia superba* I. Temperature dependence during the descent–ascent cycle. Deep-Sea Research 39A, 1177–1200.

Hofmann, E.E., Klinck, J.M., Lascara, C.M., Smith, D.A., 1996. Hydrography and circulation west of the Antarctic Peninsula and including Bransfield Strait. In: Hofmann, E.E., Quetin, L.B. (Eds.), Foundations for Ecological Research West of the Antarctic Peninsula. Antarctic Research Series, vol. 70. American Geophysical Union, Washington, DC, pp. 61–80.

Hofmann, E.E., Wiebe, P.H., Costa, D.P., Torres, J.J., 2004. An overview of the Southern Ocean Global Ocean Ecosystems Dynamics program. Deep-Sea Research II, this issue [doi:10.1016/j.dsr2.2004.08.007].

Howard, S.L., Padman, L., Hyatt, J., 2004. Mixing in the pycnocline over the western Antarctic Peninsula shelf during Southern Ocean GLOBEC. Deep-Sea Research II, this issue [doi:10.1016/j.dsr2.2004.08.002].

Jacobs, S.S., Giulivi, C.F., 1998. Interannual ocean and sea ice variability in the Ross Sea. In: Jacobs, S.S., Weiss, R.F. (Eds.), Ocean, Ice and Atmosphere Interactions at the Continental Margin. Antarctic Research Series, vol. 75. American Geophysical Union, Washington, DC, pp. 135–150.

Klinck, J.M., 1998. Heat and salt changes on the continental shelf west of the Antarctic Peninsula between January 1993 and January 1994. Journal of Geophysical Research 103, 7617–7636.

Klinck, J.M., Hofmann, E.E., Beardsley, R.C., Salihoğlu, B., Howard, S., 2004. Water-mass properties and circulation on the west Antarctic Peninsula Continental Shelf in Austral Fall and Winter 2001. Deep-Sea Research II, this issue [doi:10.1016/j.dsr2.2004.08.001].

Large, W.G., McWilliams, J.C., Doney, S.C., 1994. Oceanic vertical mixing: a review and model with a nonlocal boundary layer parameterization. Reviews of Geophysics 32, 363–403.

Levine, M.D., Padman, L., Morison, J.H., Muench, R.D., 1997. Internal waves and tides in the western Weddell Sea: observations from Ice Station Weddell. Journal of Geophysical Research 102, 1073–1089.

Marchesiello, P., McWilliams, J.C., Shchepetkin, A., 2001. Open boundary condition for long-term integration of regional oceanic models. Ocean Modelling 3, 1–20.

Markus, T., 1999. Results from an ECMWF-SSM/I forced mixed layer model of the Southern Ocean. Journal of Geophysical Research 104, 15603–15620.

Marr, J.W.S., 1962. The natural history and geography of the Antarctic krill (*Euphausia superba* Dana). Discovery Report 32, 37–465.

Martinsen, E.H., Engedahl, H., 1987. Implementation and testing of a lateral boundary scheme as an open boundary condition in a barotropic ocean model. Coastal Engineering 11, 603–627.

Mellor, G.L., Ezer, T., Oey, L.-Y., 1994. The pressure gradient conundrum of sigma coordinate ocean models. Journal of Atmospheric and Oceanic Technology 11, 1126–1134.

Mellor, G.L., Oey, L.-Y., Ezer, T., 1998. Sigma coordinate pressure gradient errors and the seamount problem. Journal of Atmospheric and Oceanic Technology 15, 1122–1131.

Milliff, R.F., Large, W.G., Morzel, J., Danabasoglu, G., Chin, T.M., 1999. Ocean general circulation model sensitivity to forcing from scatterometer winds. Journal of Geophysical Research 104, 11337–11358.

Muench, R.D., Padman, L., Howard, S.L., Fahrbach, E., 2002. Upper ocean diapycnal mixing in the northwestern Weddell Sea. Deep-Sea Research II 49, 4843–4861.

Orsi, A.H., Johnson, G.C., Bullister, J.L., 1999. Circulation, mixing, and production of Antarctic Bottom Water. Progress in Oceanography 43, 55–109.

Padman, L., Fricker, H.A., Coleman, R., Howard, S.L., Erofeeva, S., 2002. A new tidal model for the Antarctic ice shelves and seas. Annals of Glaciology 34, 247–254.

Potter, J.R., Paren, J.G., 1985. Interaction between ice shelf and ocean in George VI Sound, Antarctica. In: Jacobs, S.S. (Ed.), Oceanology of the Antarctic Continental Shelf. Antarctic Research Series, vol. 43. American Geophysical Union, Washington, DC, pp. 35–58.

Prézelin, B.B., Hofmann, E.E., Mengelt, C., Klinck, J.M., 2000. The linkage between Upper Circumpolar Deep Water (UCDW) and phytoplankton assemblages on the west Antarctic Peninsula continental shelf. Journal of Marine Research 58, 165–202.

Ross, R.M., Hofmann, E.E., Quetin, L.B., (Eds.), 1996. Foundations for Ecological Research West of the Antarctic

Peninsula. Antarctic Research Series, vol. 70. American Geophysical Union, Washington DC.

Royer, T.C., 1998. Coastal processes in the northern North Pacific. In: Robinson, A.R., Brink, K.H. (Eds.), The Sea, vol. 11, Wiley, New York, pp. 395–414.

Sciremammano Jr., F., 1979. A suggestion for the presentation of correlations and their significance levels. Journal of Physical Oceanography 9, 1273–1276.

Semtner, A.J., Chervin, R.M., 1992. Ocean general circulation from a global eddy-resolving model. Journal of Geophysical Research 97, 5493–5550.

Shchepetkin, A.F., McWilliams, J.C., 2003. A method for computing horizontal pressure-gradient force in an oceanic model with a nonaligned vertical coordinate. Journal of Geophysical Research 108, doi:10.1029/2001JC001047.

Smith, W.H., Sandwell, D.T., 1997. Global sea floor topography from satellite altimetry and ship depth soundings. Science 277, 1956–1962.

Smith, D.A., Klinck, J.M., 2002. Water properties on the west Antarctic Peninsula continental shelf: a model study of effects of surface fluxes and sea-ice. Deep-Sea Research II 49, 4863–4886.

Smith, D.A., Hofmann, E.E., Klinck, J.M., Lascara, C.M., 1999. Hydrography and circulation of the west Antarctic Peninsula continental shelf. Deep-Sea Research I 46, 925–949.

Smith Jr., W.O., Dinniman, M.S., Klinck, J.M., Hofmann, E.E., 2003. Biogeochemical climatologies of the Ross Sea, Antarctica. Deep-Sea Research II 50, 3083–3101.

Song, Y.T., 1998. A general pressure gradient formulation for ocean models. Part 1: scheme design and diagnostic analysis. Monthly Weather Review 126, 3213–3230.

Stammerjohn, S.E., Smith, R.C., 1996. Spatial and temporal variability in the west Antarctic Peninsula sea ice coverage. In: Hofmann, E.E., Quetin, L.B. (Eds.), Foundations for Ecological Research West of the Antarctic Peninsula. Antarctic Research Series, vol. 70. American Geophysical Union, Washington, DC, pp. 81–104.

Stein, M., 1992. Variability of local upwelling off the Antarctic Peninsula. Archiv für Fischereiwissenschaft 41, 131–158.

Tréguer, P., Jacques, G., 1992. Dynamics of nutrients and phytoplankton and fluxes of carbon, nitrogen and silicon in the Antarctic Ocean. Polar Biology 12, 149–162.

Wilkin, J., Hedström, K.S., 1998. User's manual for an orthogonal curvilinear grid-generation package. Technical report (available from Institute of Marine and Coastal Sciences, Rutgers University), 31pp.

Xie, P., Arkin, P.A., 1997. Global precipitation: a 17-year monthly analysis based on gauge observations, satellite estimates, and numerical model outputs. Bulletin of the American Meteorological Society 78, 2539–2558.

Zeng, X., Zhao, M., Dickinson, R.E., 1998. Intercomparison of bulk aerodynamic algorithms for the computation of sea surface fluxes using TOGA COARE and TAO data. Journal of Climate 11, 2628–2644.